

Supplementary Materials

Experimental Setup

Figure S1 shows the experiment setup schematic²². Lysing, quenching and PBS buffers are infused using an Eksigent Nanoflow LC pump (Dublin, CA) into the biochip. Red blood cells are lysed inside chip and leukocytes are preserved by introducing a quenching buffer. The leukocytes are counted electrically and specific cells CD4+/ CD8+ T cells are captured in the capture chamber as shown in Figure S1a. The electrical measurement setup is shown in Figure S1b. 5 V (rms) amplitude with 303 kHz signal is provided to the biochip's center electrode using a Zurich Instruments (Zurich, Switzerland) HF2LI lock-in amplifier. Wheatstone bridge circuit is then used with 10 k Ω resistors to measure the impedance change in between the electrodes as the cell pass²². The differential preamplifier of (Zurich Instruments) is used to take the voltage difference in between two Wheatstone branches. The resulting signal is fed to the HF2LI lock-in amplifier which measures the signal magnitude. The data is recorded at 250 kHz sampling rate using a PCIe-6351 DAQ card (National Instruments, Austin, TX)²². To take images and record videos of the cells flowing through the channels in the biochip, a Nikon Eclipse E600 FN microscope (Nikon Instruments, Incl. Melville, NY) and a Phantom v310 (Vision Research, Wayne, NJ) high speed camera was used²².

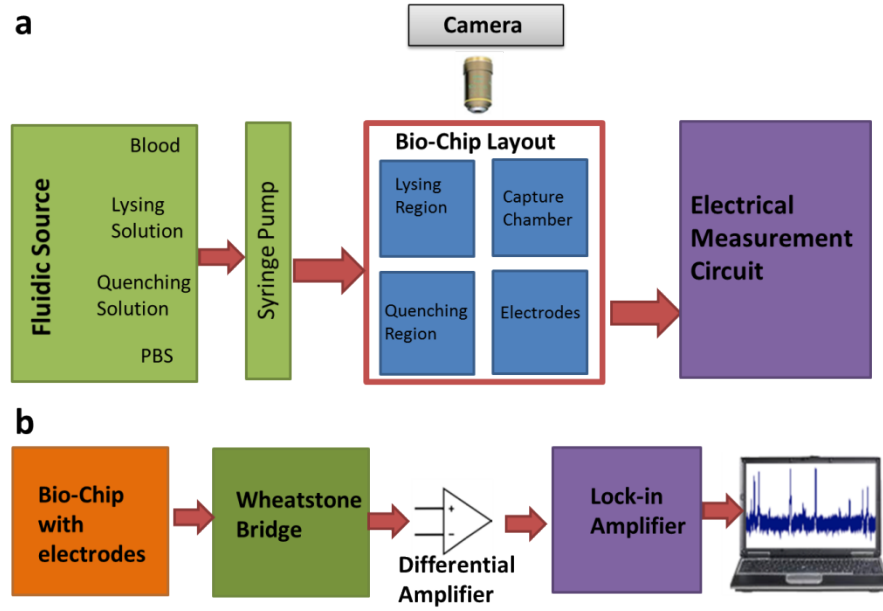


Fig. S1: (a) Schematic of the experimental setup. Its shows the fluidic sources, syringe pump, biochip, camera, and electrical measurement circuit. (b) The components of the electrical measurement circuit.

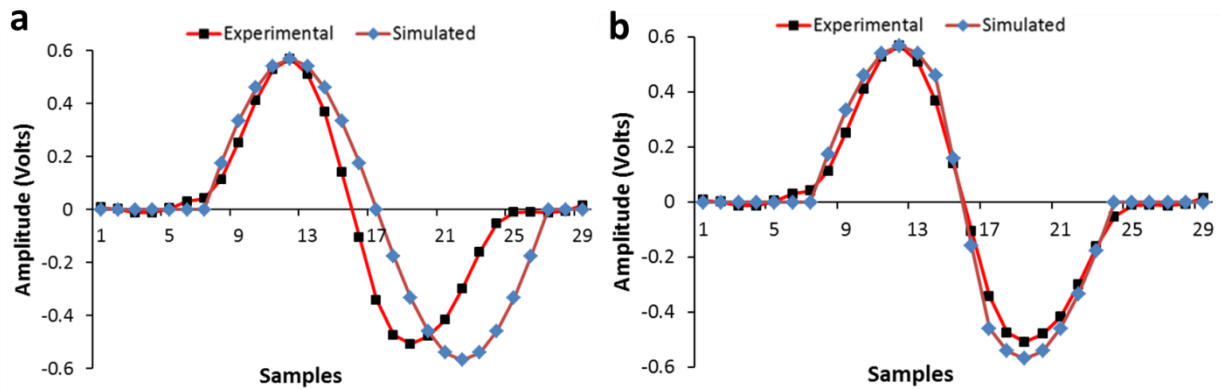


Fig. S2: Comparison of simulated and experimental electrical pulse of a cell. (a) A cell is modelled as a simple sinusoid while not considering the pulse overlap at the middle electrode and compared with the electrical pulse. (b) Comparison of the simulated and experimental electrical cell pulse shows the difference in between the negative pulse amplitudes.

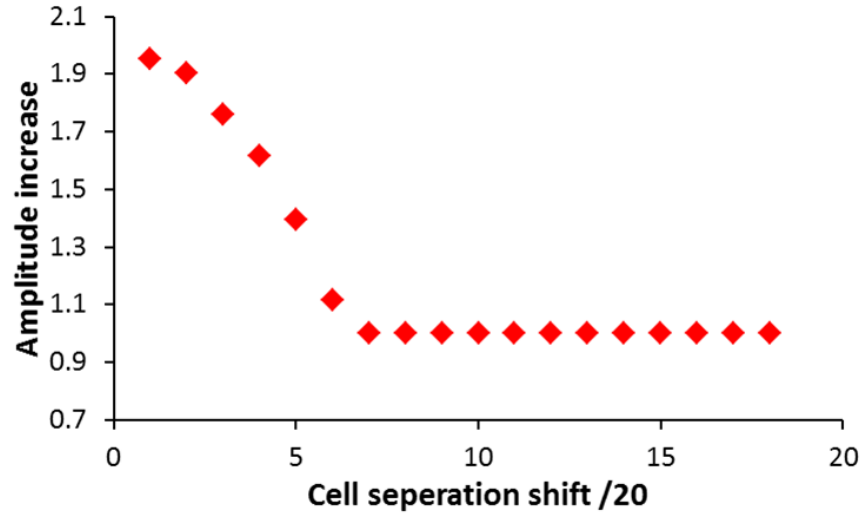


Fig. S3: The increase in the amplitude of the positive peak of cell pulse with varying shift values for the occurrence of the second coincidence cell. The change in amplitude happens only for the coincidence Type 1 range.

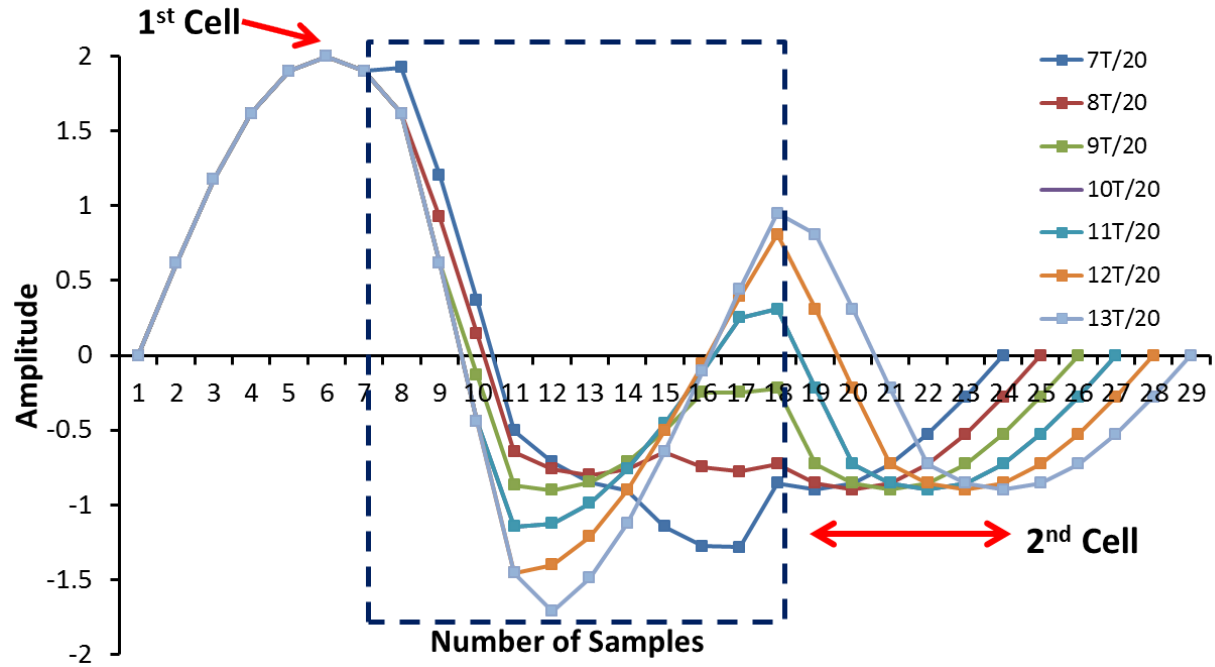


Fig. S4: The simulated cell pulses for the entire time delay range of $\left(\frac{6T}{20} \text{ to } \frac{13T}{20}\right]$ of type 2 coincidence when the second cell equal the size of first cell ($2A_2 = A_1$) enters the detection region.

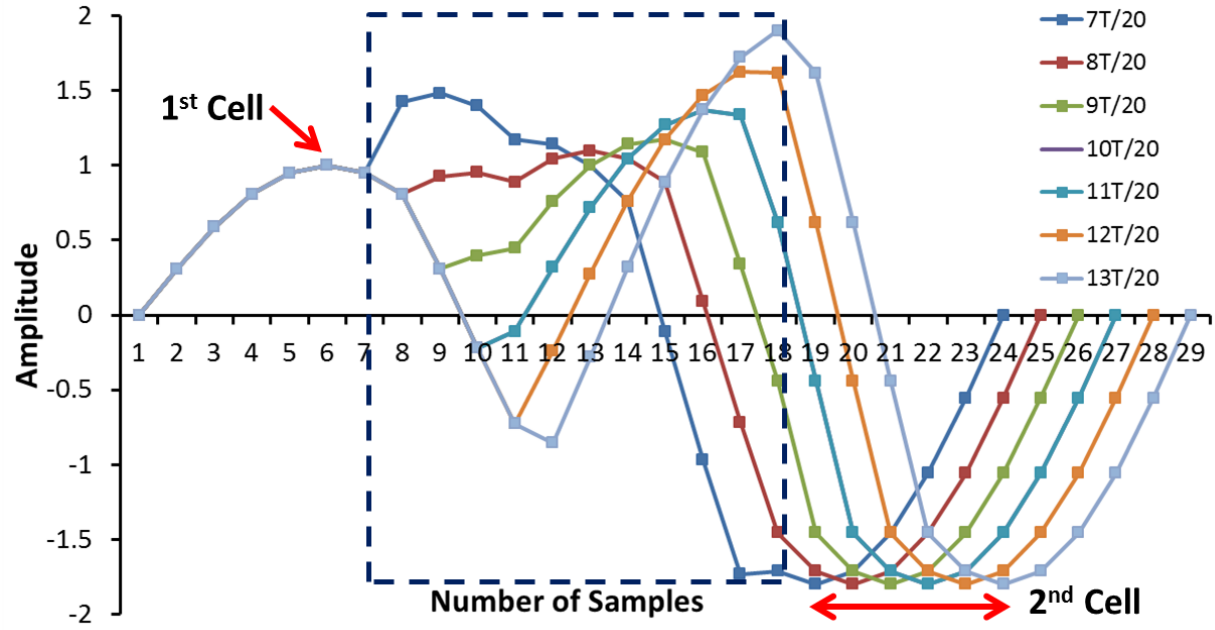


Fig. S5: The simulated cell pulses for the entire time delay range of $\left(\frac{6T}{20} \text{ to } \frac{13T}{20}\right]$ of type 2 coincidence when the second cell equal the size of first cell ($A_2 = 2A_1$) enters the detection region.

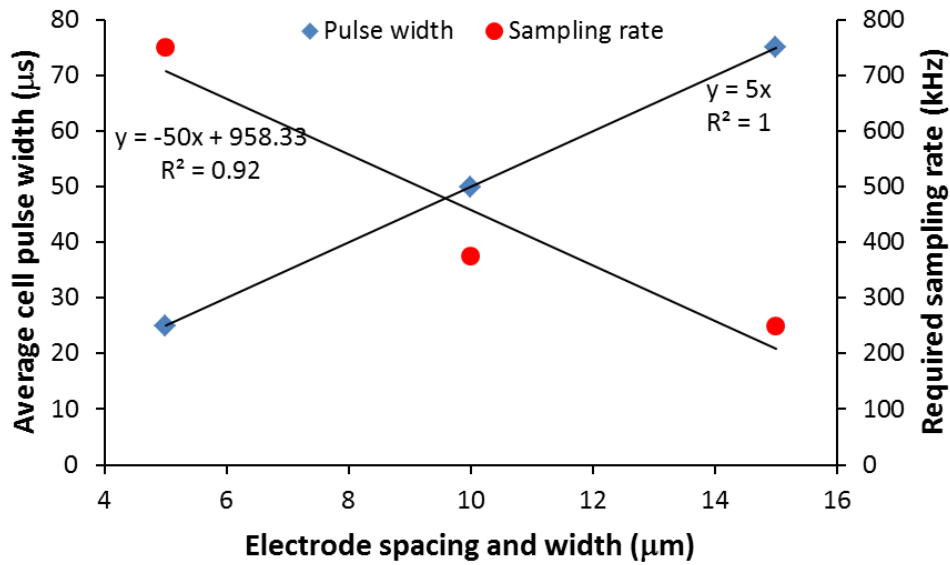


Fig. S6: The width of the cell pulse would reduce as the electrode spacing and width reduce. In order to get the same number of samples to get optimum resolution the sampling rate needs to be increased.

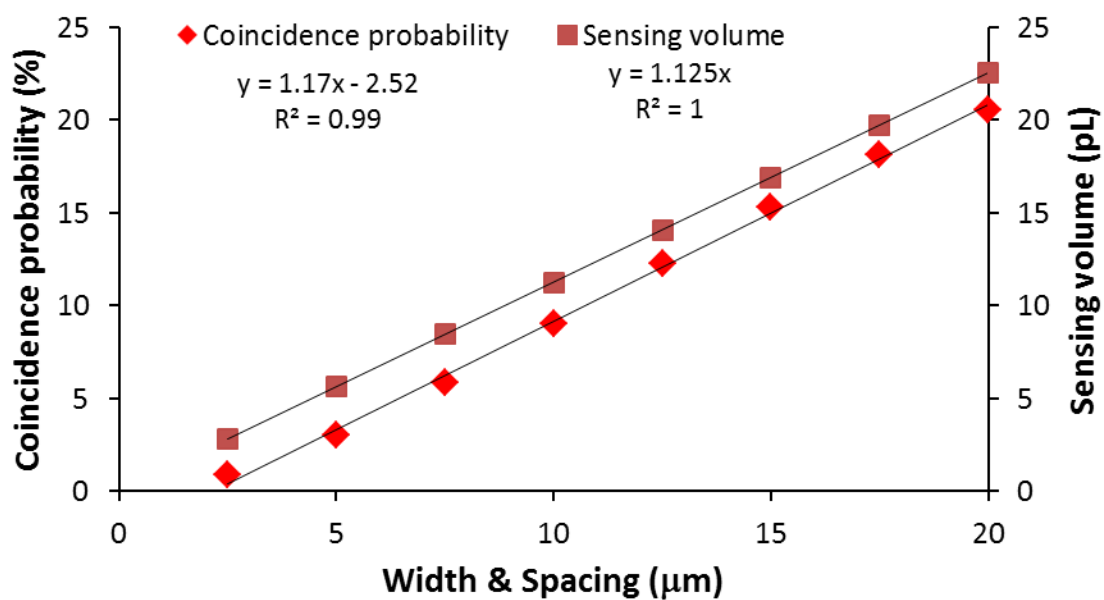


Fig. S7: The coincidence probability with varying width & spacing of the electrodes. The probability decreases linearly as the width and electrode spacing is reduced. The secondary axis shows the corresponding sensing volume.